nature neuroscience

Retrograde activation of presynaptic NMDA receptors enhances GABA release at cerebellar interneuron–Purkinje cell synapses

Ian C Duguid & Trevor G Smart

Synaptic inhibition is a vital component in the control of cell excitability within the brain. Here we report a newly identified form of inhibitory synaptic plasticity, termed depolarization-induced potentiation of inhibition, in rodents. This mechanism strongly potentiated synaptic transmission from interneurons to Purkinje cells after the termination of depolarization-induced suppression of inhibition. It was triggered by an elevation of Ca^{2+} in Purkinje cells and the subsequent retrograde activation of presynaptic NMDA receptors. These glutamate receptors promoted the spontaneous release of Ca^{2+} from presynaptic ryanodine-sensitive Ca^{2+} stores. Thus, NMDA receptor–mediated facilitation of transmission at this synapse provides a regulatory mechanism that can dynamically alter the synaptic efficacy at inhibitory synapses.

Synaptic $GABA_A$ receptors are vital for fast inhibitory neurotransmission in the CNS. Regulating the function of these receptors is therefore crucial to the control of neuronal excitability. In principle, this can be achieved either by modifying the receptor's response to GABA or by influencing the presynaptic release of GABA. With regard to transmitter release, retrograde signaling provides an efficient feedback mechanism that enables postsynaptic neurons to control their presynaptic inputs, as, for example, during depolarization-induced suppression of inhibition (DSI)[1,2]. Repetitive depolarization of cerebellar Purkinje or hippocampal CA1 neurons increases postsynaptic Ca^{2+}, initiating the retrograde release of endocannabinoids. These compounds then activate presynaptic CB1 receptors, suppressing the release of GABA[3,4]. A similar mechanism operates during depolarization-induced suppression of excitation (DSE)[5]. During DSI and DSE, presynaptic CB1 receptor activation reduces both the probability of transmitter release and the overall synaptic efficacy for tens of seconds after the initial stimulation[3–7]. Here, we describe a new retrograde signaling pathway that regulates GABA release in the cerebellum by identifying a long-lasting, profound depolarization-induced potentiation of inhibition (DPI) that occurs after the termination of DSI.

Retrograde neurotransmission is thought to operate at various synapses throughout the brain to modulate presynaptic transmitter release[8–12]. How this modulation is manifest depends on the type of retrograde transmitter, the target presynaptic receptor and the type of cell upon which the receptors reside. In this context, glutamate has been proposed as a stimulus-evoked retrograde messenger in the cerebellum that may activate both ionotropic and metabotropic glutamate receptors (mGluR) on excitatory and inhibitory terminals[11]. The existence of presynaptic NMDA receptors[13,14] implies that they could play a key role in the induction of synaptic plasticity—for example, in cerebellar long-term depression (LTD)[15]. Indeed, presynaptic NMDA receptors may also modulate the release of GABA at the interneuron–Purkinje cell (IN-PC) synapse[16]; however, their impact on the induction of cerebellar inhibitory synaptic plasticity is unknown.

In this study, we report that physiological stimuli can induce a potentiation of inhibitory synaptic transmission at the IN-PC synapse, defined as DPI. This glutamate-mediated retrograde potentiation of inhibition requires an increase in postsynaptic Ca^{2+} and can be evoked by the stimulation of climbing fibers, similar to what is observed *in vivo*[17,18]. DPI can also be reproduced by direct activation of NMDA receptors (which are located at putative presynaptic axon terminals on basket/stellate cells) and prevented by inhibition of these receptors. After NMDA receptor activation, the release of Ca^{2+} from presynaptic ryanodine-sensitive stores is facilitated, causing a sustained increase in inhibitory synaptic efficacy at the IN-PC synapse. The discovery of DPI, in conjunction with the widespread distribution of presynaptic ionotropic glutamate receptors, may be indicative of a more general role for the retrograde release of glutamate and presynaptic NMDA receptors in the potentiation of inhibitory synaptic transmission in the CNS.

RESULTS

Depolarization-induced potentiation of inhibition

We studied inhibitory synaptic plasticity during early cerebellar development using whole-cell recording from Purkinje cells at postnatal days (P) 6–8. To induce plasticity, we applied a single train of depolarizing voltage steps (0.8-s total duration of depolarization; see Methods) to Purkinje cells voltage clamped at –70 mV. This induces

Department of Pharmacology, University College London, Gower Street, London WC1E 6BT, UK. Correspondence should be addressed to T.G.S. (t.smart@ucl.ac.uk).

Published online 18 April 2004; doi:10.1038/nn1227

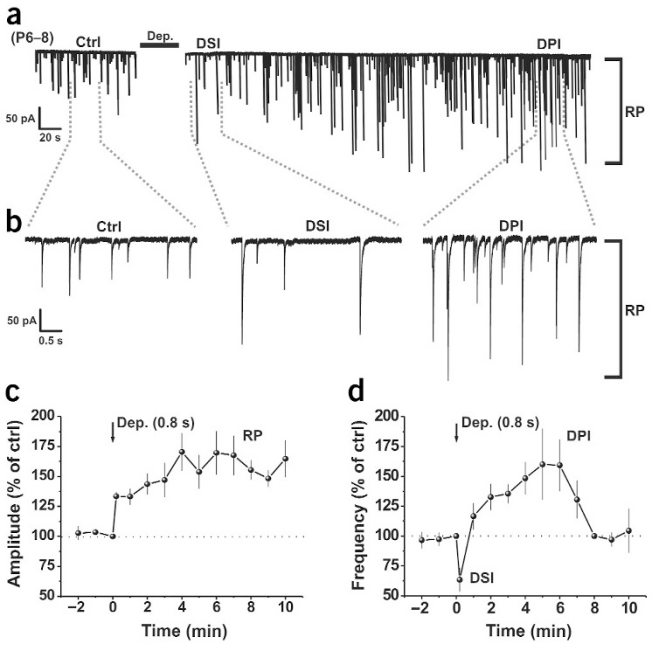

Figure 1 Postsynaptic depolarization induces DSI, rebound potentiation and DPI in P6–8 cerebellar Purkinje cells. (**a**) Continuous recordings of mIPSCs in control aCSF and after a train of conditioning stimuli (Dep, +70 mV, 100 ms, 0.5 Hz, eight stimuli). (**b**) High-resolution mIPSC recordings (selected from **a**) during control (before stimulation), during peak DSI and after onset of DPI, which occur with rebound potentiation (RP). (**c**,**d**) Normalized mean mIPSC amplitudes (**c**) and frequencies (**d**; $n = 7$). Dotted line and arrows here and in other figures represent the baseline levels (100%) before the stimulus and the point of stimulus induction ($t = 0$ min), respectively. Throughout, all data points represent means ± s.e.m.

large dendritic Ca^{2+} transients similar to those evoked by climbing fiber stimulation[19–21] and is a key prerequisite for the induction of various forms of inhibitory synaptic plasticity[19,22–24]. To assess the sensitivity of postsynaptic $GABA_A$ receptors and the extent of spontaneous presynaptic GABA release, we measured both the amplitudes and frequencies of miniature inhibitory postsynaptic currents (mIPSCs) in the presence of the Na^+ channel blocker tetrodotoxin (TTX; 500 nM) and the AMPA receptor antagonist 2,3-dioxo-6-nitro-1,2,3,4-tetrahydrobenzo(f)quinoxaline-7-sulfonamide (NBQX; 10 M). Direct Purkinje cell depolarization potentiated the mean mIPSC amplitude to 154 ± 14% (control mIPSC amplitude measured before depolarization = 100%), at 5 min after stimulus ($n = 7$), in accord with the development of rebound potentiation[1,19] (**Fig. 1a–c**). As expected, after cessation of the stimulus the mean mIPSC frequency was reduced by the induction of DSI[3,4,7] (63 ± 10%, control frequency 100%; $n = 7$; **Fig. 1a**,**b**,**d**). However, as DSI began to dissipate after the stimulus ($\Delta t = 1$ min), we observed a robust increase in the mean mIPSC frequency (159 ± 22%, $\Delta t = 6$ min; $n = 7$), which returned to baseline ~8 min after the stimulus (**Fig. 1a**,**b**,**d**). The increased mIPSC frequency appeared as a new plasticity phenomenon at this synapse and was subsequently defined as a depolarization-induced potentiation of inhibition.

During the first 2 weeks of postnatal development, the cerebellum undergoes considerable maturation and synaptogenesis[25,26]. We assessed whether DPI was maintained during the latter stages of this period using P11–14 slices. Notably, the depolarizing protocol used in the P6–8 slices did not induce DPI at P11–14 (98 ± 3%, $\Delta t = 5$ min; $n = 6$; **Fig. 2a**). However, we observed rebound potentiation in each cell (**Fig. 2a**, inset), indicating that rebound potentiation and DPI are discrete forms of inhibitory synaptic plasticity, probably involving separate signaling pathways. The failure to induce DPI may result from a reduced availability of intracellular Ca^{2+} owing to increased expression of Ca^{2+} binding proteins in older Purkinje cells. This explanation would also account for the lower magnitude of DSI in P11–14 (87 ± 2%, $n = 6$; **Fig. 2a**) as compared to P6–8 Purkinje cells (**Fig. 1d**). Any increased Ca^{2+} sequestration at P11–14 was obviated by promoting Ca^{2+} entry with an increased depolarization of the Purkinje cell from 0.8 s to 2 s. This longer stimulus evoked increased DSI (63 ± 4%) and a small DPI (120 ± 6%, $\Delta t = 5$ min; $n = 6$) that lasted for ~10 min (**Fig. 2b**,**d**). Increasing the stimulus duration still further, to 5 s, induced both robust DSI (61 ± 7%) and increased DPI (155 ± 15%, $\Delta t = 5$ min; $n = 9$), the latter persisting for more than 15 min (**Fig. 2c**,**d**). Concurrently with the modulation of mIPSC frequency, lengthening the stimulus duration also increased the magnitude of rebound potentiation from 144 ± 4% (0.8 s) to 156 ± 8% (2 s) and 170 ± 11% (5 s), respectively, at $\Delta t = 5$ min ($n = 6$, 6 and 9; **Fig. 2a–c**, insets). These results indicated that cerebellar maturation enforces a strict control over the induction of DPI.

We next investigated whether the induction of DPI could also affect action potential–dependent inhibitory synaptic transmission. In each P11–14 Purkinje cell, applying a depolarizing protocol (5 s) in the absence of Na^+ channel blockers induced robust DSI, rebound potentiation and DPI, similar in their magnitudes to those observed with action potential–independent GABA release (**Table 1**). Taken overall, DPI affects both action potential–dependent and –independent forms of inhibitory neurotransmission, implying that similar signaling pathways are involved.

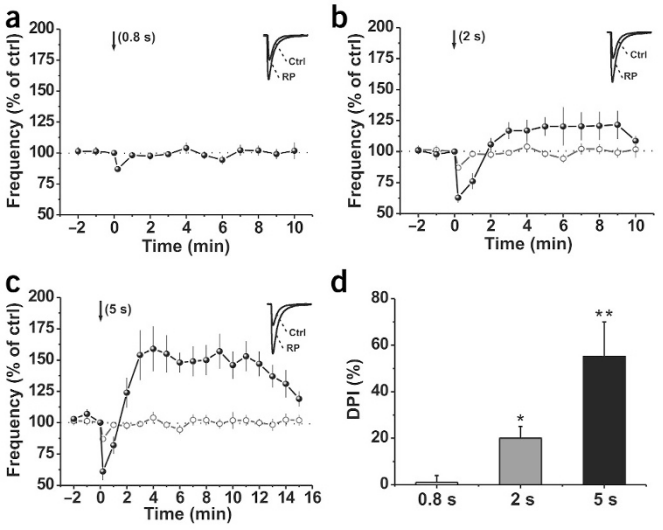

Figure 2 DPI in P11–14 cerebellar Purkinje cells. (**a**–**c**) Normalized mean mIPSC frequencies (black circles) before and after the following conditioning stimuli: 100-ms duration, 0.5 Hz, repeated eight times ($n = 6$; **a**); 2-s duration, single pulse ($n = 6$; **b**); or 5-s duration, single pulse ($n = 9$; **c**). Open circles in **b** and **c** represent data taken from **a** for comparison. Insets in **a**–**c** show superimposed mean mIPSCs from 50 consecutive events recorded in control (Ctrl) and 5 min after stimulus cessation during rebound potentiation. (**d**) Bar graph of the relative mIPSC frequency increase (DPI, %) over controls (set to 0%) measured at 4–5 min after induction by 0.8, 2 and 5 s conditioning stimuli. $^*P < 0.05$, $^{**}P < 0.01$.

Climbing fiber stimulation induces DPI

To determine whether DPI was physiologically relevant and could be evoked after synaptic activity, we recorded from P11–14 Purkinje cells in artificial cerebrospinal fluid (aCSF) without TTX and NBQX, using a K^+-based pipette solution, while stimulating distinct climbing fiber synaptic inputs. We stimulated climbing fiber inputs at 2 Hz for 5 s (**Fig. 3a**) to reproduce their intrinsically low *in vivo* firing rate[17,18] and to match the stimulus duration that induced DPI in P11–14 Purkinje cells (**Fig. 2c,d**). As determined using current-clamp recording, each stimulated climbing fiber input induced a typical complex spike (**Fig. 3b**) with a profile characteristic of a large Ca^{2+} influx into the Purkinje cell dendrites[19,20,27,28]. Furthermore, voltage-clamped EPSCs showed substantial paired-pulse depression, reflecting the high probability of release at this synapse[29] (**Fig. 3c**). Repetitive climbing fiber stimulation of Purkinje cells resulted in the induction of DSI (81 ± 4%) and DPI (140 ± 4%, Δt = 5 min; n = 5; **Fig. 3d,e**). Both DSI and DPI were similar in magnitude and duration to those induced by direct Purkinje cell depolarization (5 s) using a Cs^+-based pipette solution (compare **Fig. 2c** and **Table 1**). In all cells examined with climbing fiber stimulation, the mean sIPSC amplitude increased to 150 ± 6% (Δt = 5 min; n = 5; **Fig. 3e**, inset). To address whether DPI, after climbing fiber stimulation, could have resulted from the direct 'spillover' of glutamate from climbing fiber axon terminals, we perfused the Ca^{2+} chelator BAPTA (30 mM) into Purkinje cells. This completely blocked the induction of DPI by climbing fiber stimulation, indicating that glutamate spillover cannot be involved in this process (**Fig. 3f**). Taken together, these data show that identical forms of DPI can be induced either using physiological climbing fiber stimulation or under the more controlled conditions of direct somatic depolarization, thereby increasing synaptic efficacy at the IN-PC synapse for several minutes.

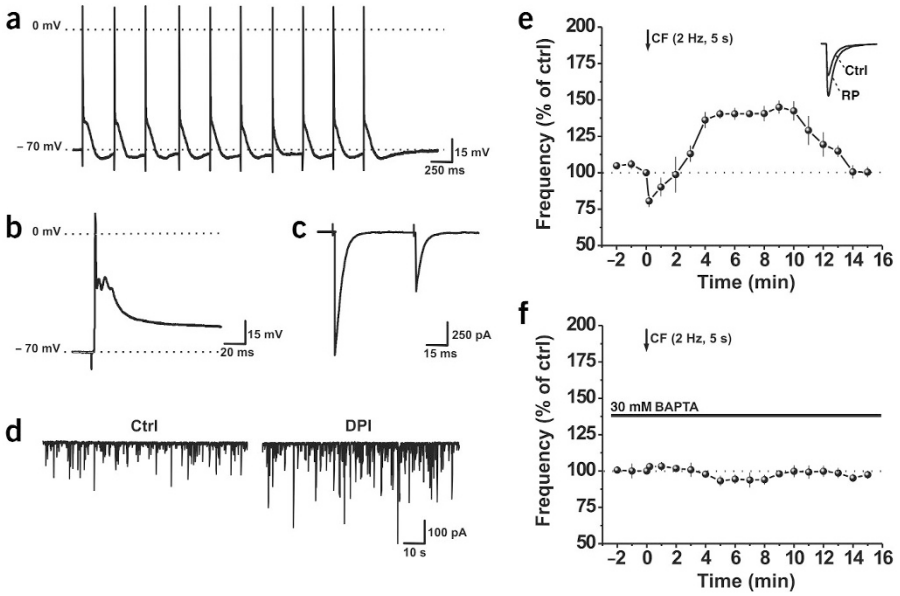

Figure 3 Physiological climbing fiber (CF) stimulation induces DPI in P11–14 Purkinje cells. (**a**) Continuous current-clamp recording of a series of complex spikes generated by repetitive CF stimulation (2 Hz, 5 s). (**b**) Higher time resolution of a typical complex spike. (**c**) Typical paired-pulse EPSCs (50-ms interval) evoked by CF stimulation. (**d**) Spontaneous IPSCs, recorded with a K^+-based pipette solution, in control aCSF (Ctrl) and after CF stimulation (DPI; 2 Hz, 5 s). (**e**) Normalized mean sIPSC frequency before and after CF stimulation (2 Hz, 5 s; n = 5). Inset, superimposed mean sIPSCs (of 50 consecutive events) recorded in control and 5 min after CF stimulation during rebound potentiation. (**f**) Normalized mean sIPSC frequency before and after CF stimulation (2 Hz, 5 s) in Purkinje cells internally perfused with 30 mM BAPTA (n = 5).

Calcium dependence and presynaptic DPI expression

Internal perfusion of Purkinje cells with BAPTA (30 mM) prevented the induction of both DSI and DPI in either P6–8 or P11–14 slices after direct depolarization (n = 5; **Fig. 4a,b**). This joint dependence on postsynaptic Ca^{2+} may underlie the significant correlation (r^2 = 0.93; n = 30) between the magnitudes of DSI and DPI in every Purkinje cell examined (**Fig. 4c**). The increased frequency of mIPSCs and sIPSCs during DPI implied that this is a presynaptic phenomenon, a conclusion supported by the paired-pulse ratios (50-ms interval) determined from the amplitudes of successively evoked IPSCs during DPI. A change in the paired-pulse ratio is presumed to reflect a modification to the probability of transmitter release at that synapse. Similar to previous findings[16,30], evoked IPSCs from P11–14 slices showed paired-pulse depression during control recordings (0.73 ± 0.08; n = 7). By comparison, the induction of DSI was accompanied by an increased paired-pulse ratio (1.11 ± 0.07, Δt = 1 – 40 s; n = 7), which is in accord with a reduced release probability[7,31]. However, during DPI, the paired-pulse ratio was significantly lower than in the control recordings (0.5 ± 0.07, Δt = 5 min; n = 7; **Fig. 4d,e**), reflecting an increase in the probability of release at the IN-PC synapse. The presynaptic nature of DPI was further emphasized by examining the coefficient of variation (c.v.) for evoked IPSC amplitudes. After direct Purkinje cell depolarization, the transformed coefficient of variation ($1/c.v.^2$) for evoked IPSCs significantly decreased during DSI and increased during DPI (**Fig. 4f**; n = 5). The paired-pulse ratios and c.v. values for evoked IPSCs, together with the frequencies of mIPSCs and sIPSCs, strongly implied that DPI is presynaptic in origin.

Presynaptic NMDA receptors mediate DPI

The molecules mediating DPI are presumed to act on specific receptors located on presynaptic axon terminals of basket/stellate cells. Previously, both glutamate and endocannabinoids have been proposed as retrograde messengers in the cerebellum[4,5,11,31,32]. We therefore examined their putative effects using selective receptor antagonists. As expected, the induction of DSI by direct somatic depolarization in P6–8 and P11–14 Purkinje cells was abolished by the CB1 receptor antagonist SR141716A (1 M; **Fig. 5a**; n = 5 and 6). However, DPI was unaffected by either SR141716A (1 M; n = 5

Table 1 DPI induction affects both action potential–dependent and –independent GABA release

	Peak DSI		Peak DPI		
	Amplitude	Frequency	Amplitude	Frequency	*n*
mIPSCs	135 ± 7%	61 ± 7%	170 ± 11%	155 ± 15%	9
sIPSCs	85 ± 11%	71 ± 4%	171 ± 10%	152 ± 10%	5

Peak DSI was calculated during the initial 20s after stimulus. Peak DPI was calculated at Δt = 5 min after stimulus. Values given are mean ± s.e.m. and all values are statistically significant from control (100%). Paired Student's t-test, $P < 0.01$.

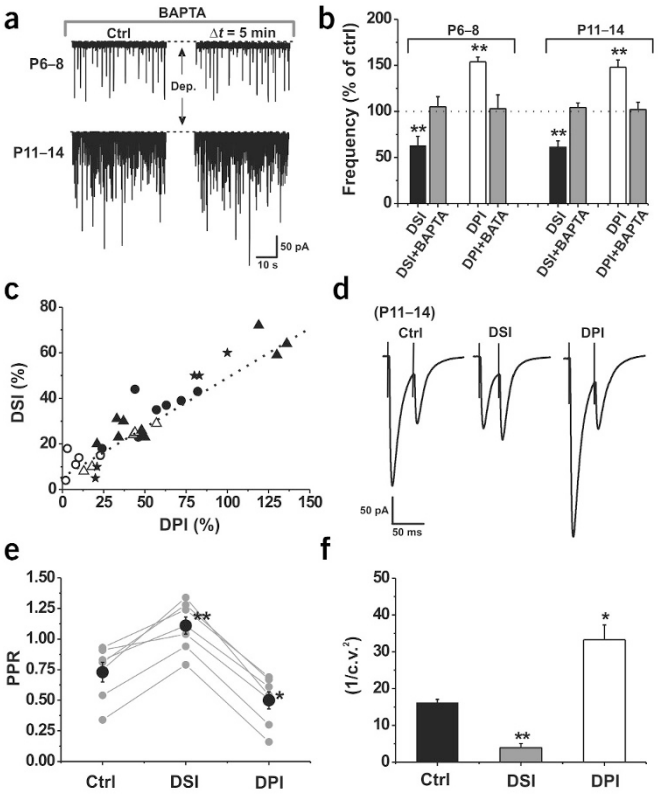

Figure 4 Calcium-dependent release of a retrograde messenger and the presynaptic origin of DPI. (**a**) mIPSC recordings from P6–8 and P11–14 Purkinje cells before and after depolarization (P6–8, 0.8 s; P11–14, 5 s) in the presence of 30 mM intracellular BAPTA. (**b**) Modulation of mean mIPSC frequencies in P6–8 and P11–14 slices during peak DSI (black bars) and peak DPI (open bars) in the absence ($n = 7$ and 6, respectively) and presence of 30 mM internal BAPTA (gray bars, $n = 5$). (**c**) Relationship between the percentage magnitudes of DSI and DPI, induced by different stimuli, and recorded from the same cells for P6–8 (0.8 s, filled stars; $n = 5$); P11–14 (0.8 s, open circles; $n = 5$); P11–14 (5 s, filled triangles; $n = 9$); P11–14 (climbing fiber (CF), 2 Hz, 5 s; open triangles; $n = 5$); and P11–14 slices (5 s, sIPSCs; filled circles; $n = 6$). (**d**) Examples of paired IPSCs (50-ms interval) recorded in P11–14 Purkinje cells before (Ctrl), immediately after (DSI), and 5 min after application of a 5-s conditioning stimulus (DPI). (**e**) Changes in paired-pulse ratio during DSI and DPI ($n = 7$). Data from the same Purkinje cells (gray circles) are connected by straight lines. Black circles, means ± s.e.m. (**f**) Bar graph showing changes in the transformed coefficient of variation (1/c.v.^{2}) of evoked IPSC amplitudes during DSI and DPI ($n = 5$). $^*P < 0.05$, $^{**}P < 0.01$.

and 6) or the metabotropic glutamate receptor (mGluR) antagonist LY341495, applied at a concentration (200 nM) that is selective for presynaptic group II mGluRs[33] ($n = 5$ and 5; **Fig. 5b**). In contrast, the involvement of NMDA receptors was strongly and specifically implicated in DPI. Irrespective of whether DPI was induced by direct (5 s) depolarization or by climbing fiber stimulation, the selective antagonist D-APV (50 M) abolished the increased IPSC frequencies in P6–8 (0.8 s, 101 ± 13%, $\Delta t = 5$ min; $n = 5$) and P11–14 slices (5 s, 101 ± 3% and climbing fiber, 101 ± 7%, $\Delta t = 5$ min; $n = 5$; **Fig. 5c–e**). In comparison, the induction of rebound potentiation was not affected by any of these antagonists, indicating that this plasticity phenomenon is discrete from DPI. Overall, this indicates that Purkinje cell depolarization may induce retrograde release of either glutamate or glutamate-like molecules, which then activate presynaptic NMDA receptors to enhance the release of GABA at the IN-PC synapse. If glutamate were released by Purkinje cell depolarization, it would rapidly be sequestered by surrounding excitatory amino acid transporters (EAATs), which might explain the lack of DPI observed in P11–14 Purkinje cells after modest depolarization (0.8 s). To examine this possibility, we isolated DPI by blocking DSI using SR141716A (1 M) and then simultaneously blocked EAATs with THA (200 M). The previously subthreshold stimulation (0.8 s) now resulted in the induction of a robust DPI (125 ± 8%, $\Delta t = 3$ min; $n = 5$), which was blocked by D-APV (50 M; **Fig. 5f**). These results indicate that even with modest Purkinje cell depolarization, glutamate is released into the extracellular space before being rapidly sequestered by EAATs. Therefore, increasing the stimulus duration will presumably cause increased levels of released glutamate to transiently saturate the EAATs. This will then facilitate presynaptic NMDA receptor activation and the induction of DPI.

The duration of stimulus required to evoke heterosynaptic DPI (and DSI[23]) was of the order of several hundred milliseconds; however, whether brief activation of presynaptic NMDA receptors is sufficient to induce DPI was uncertain. Bath application of NMDA for 3–6 min increases mIPSC frequency[16], but such long applications may overestimate the NMDA receptor–mediated effect. We therefore attempted to reproduce DPI by briefly activating presynaptic NMDA receptors through pressure application of NMDA (50 M) to the Purkinje cell dendritic field in P11–14 slices in the presence of 1 mM Mg^{2+} (**Fig. 6a,b**). This caused an immediate increase in mIPSC frequency (310 ± 33%), which subsided (156 ± 14%, $\Delta t = 5$ min) before slowly returning to control levels (105 ± 5%, $\Delta t = 13$ min; $n = 5$; **Fig. 6c**). We discounted any NMDA receptor activation in Purkinje cells during the induction of DPI, because no NMDA-induced current was observed (**Fig. 6b**), emphasizing the lack of any functional NMDA receptors in these cells[16,34]. Our results indicated that brief activation of presynaptic NMDA receptors is sufficient to induce a sustained elevation in spontaneous GABA release at the IN-PC synapse.

Although the existence of presynaptic NMDA receptors *per se* has been reported[14–16,35], their presence on cerebellar interneuron axon terminals has not been explored. We addressed this by using triple immunolabeling for the NMDA receptor subunits, NR1 and the NR2A–D splice variants, together with synaptophysin and glutamic acid decarboxylase ($GAD_{65/67}$) as markers for presynaptic release sites on inhibitory axon terminals. Examination of the basket/stellate cell axons showed evidence of triple colocalization, specifically on axon varicosities where high densities of NR1 (**Fig. 6d**) and all the NR2 subunits are present (NR2A is shown as the example; **Fig. 6e**). Our results support the hypothesis that functional presynaptic NMDA receptors, expressed on axon terminals of cerebellar basket/stellate cells, are key components for the induction of DPI.

Presynaptic calcium channels and stores in DPI

We next examined whether the sustained increase in GABA release required NMDA receptor activation alone or relied on voltage-dependent Ca^{2+} channels recruited after depolarization of the axon terminals. Although 100 M Cd^{2+} blocked action potential–evoked GABA release onto Purkinje cells (control, mean sIPSC + mIPSC amplitude, 360 ± 41 pA and frequency 10 ± 1 Hz; +Cd^{2+}, 118 ± 5 pA and 3 ± 0.6 Hz), as expected[36], it did not affect the sustained increase in mIPSC frequency after NMDA application (147 ± 6%, $\Delta t = 5$ min; $n = 5$; **Fig. 7a**), indicating that voltage-dependent Ca^{2+} channels have no role in DPI. Cadmium ions can partially block NMDA receptors[37], but this effect was relatively insignificant in our

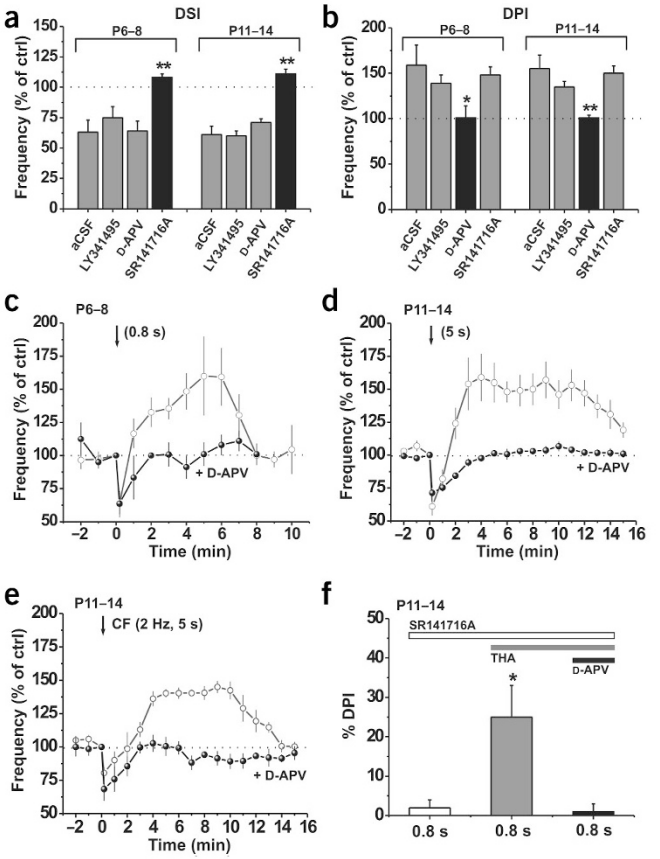

Figure 5 Presynaptic NMDA receptors mediate DPI in cerebellar Purkinje cells. (**a**,**b**) Bar graphs of mean mIPSC frequencies in P6–8 and P11–14 Purkinje cells during DSI (**a**) and DPI (**b**; $\Delta t = 5$ min), in the absence (aCSF, $n = 7$ and 9) or presence of: 200 nM LY341495 ($n = 5$), 50 M D-APV ($n = 5$) and 1 M SR141716A ($n = 5$ and 6). (**c**–**e**) Normalized mean mIPSC (**c**,**d**) and sIPSC frequencies (**e**) before and after application of a conditioning stimulus to P6–8 (**c**) and P11–14 Purkinje cells (**d**,**e**) in control aCSF (open circles, $n = 7$, 9 and 5, respectively) and in the presence of 50 M D-APV (black circles, $n = 5$, 5 and 5, respectively). (**f**) Bar graph of the relative mIPSC frequency increase (DPI, %) caused by a subthreshold stimulus (0.8 s) to P11–14 Purkinje cells in the presence of 1 M SR141716A (open bar, $n = 4$); 1 M SR141716A and 200 M THA (gray bar, $n = 5$); or 1 M SR141716A, 200 M THA and 50 M D-APV (black bar, $n = 5$). $^*P < 0.05$.

study, with 100 M Cd^{2+} inhibiting 50 M NMDA responses in interneurons by only 11 ± 2% ($n = 6$).

Given that presynaptic ryanodine-sensitive Ca^{2+} stores may mediate spontaneous transmitter release[38,39] and that residual presynaptic Ca^{2+} is crucial for some forms of short-term plasticity[40], it was plausible that axonal Ca^{2+} stores might also support DPI. To determine whether presynaptic ryanodine receptors were required, we pressure applied NMDA (50 M) to P11–14 Purkinje cells in the presence of 100 M ryanodine, a concentration sufficient to block ryanodine receptors[38,41]. During NMDA application, ryanodine markedly attenuated the mIPSC frequency peak potentiation to 140 ± 10% ($n = 5$). Notably, the increased mIPSC frequency was not maintained, returning to baseline within 2 min (101 ± 5%, $\Delta t = 3$ min; $n = 5$; **Fig. 7b**). Ryanodine also reduced the basal mIPSC amplitude (by ~30%) and frequency (by ~50%) in unstimulated Purkinje cells, demonstrating that presynaptic ryanodine receptors are required during spontaneous GABA release[38]. These findings indicated that NMDA receptor–mediated entry of Ca^{2+} into axonal boutons may be insufficient to evoke a sustained increase in GABA release at the IN-PC synapse. The increased release may therefore be dependent on Ca^{2+}-induced Ca^{2+} release (CICR) from presynaptic ryanodine-sensitive stores, which amplify the initial rise in bouton Ca^{2+}, thus inducing the sustained release component that typifies DPI.

To explore this hypothesis, we depolarized Purkinje cells in the presence of ryanodine (100 M). However, local application of ryanodine blocks both pre- and postsynaptic Ca^{2+} release from intracellular stores. In consequence, we observed reductions in the postsynaptic Ca^{2+}-dependent induction of DSI, DPI and rebound potentiation. Therefore, to differentiate the role of the presynaptic Ca^{2+} stores during DPI induction, we applied a depolarizing stimulus (5 s) to P11–14 Purkinje cells in the presence of ryanodine (100 M) while compensating for the blocked postsynaptic ryanodine receptors. This compensation involved dialyzing the Purkinje cell with caged Ca^{2+} retained in the photolabile chelator nitrophenyl-EGTA. Postsynaptic Ca^{2+} was uncaged by rapid flash photolysis in a process designed to mimic the release of Ca^{2+} from intracellular stores. Application of this compensated conditioning stimulus in the presence of 100 M ryanodine resulted in the induction of DSI and a rebound potentiation of similar magnitude to that observed under control conditions (DSI, 56 ± 6%; rebound potentiation, 155 ± 8%, $\Delta t = 5$ min; $n = 6$; **Fig. 7c** and inset), indicating that postsynaptic Ca^{2+} dynamics were largely unaffected by ryanodine. However, the same conditioning stimulus did not induce DPI (92 ± 3%, $\Delta t = 6$ min; $n = 6$; **Fig. 7c**), indicating that presynaptic ryanodine-sensitive Ca^{2+} stores are likely to have a pivotal role in maintaining the increased GABA release during DPI.

DPI and synaptic charge transfer at IN-PC synapses

To understand the functional consequences of inducing DPI and rebound potentiation, we measured the synaptic charge transfer as an indicator of synaptic efficacy. By inhibiting DPI with D-APV, the increase in postsynaptic $GABA_A$ receptor responsiveness caused by rebound potentiation[19,42] potentiated the mean charge transfer by 79 ± 9% ($n = 5$) for mIPSCs and by 45 ± 9% ($n = 5$) for sIPSCs, as compared to controls (**Fig. 7d**). When rebound potentiation and DPI were induced together, the mean synaptic charge transfer increased by 209 ± 32% ($n = 8$) and 205 ± 36% ($n = 6$) for mIPSCs and sIPSCS, respectively (**Fig. 7d**). These values indicate that DPI markedly enhances synaptic charge transfer and overall synaptic efficacy at the IN-PC synapse beyond that resulting from rebound potentiation alone.

DISCUSSION

In this study we have identified a new form of inhibitory synaptic plasticity that we term depolarization-induced potentiation of inhibition. For induction, DPI requires a rapid rise in postsynaptic Ca^{2+} in the Purkinje cell and subsequent retrograde release of glutamate that diffuses to presynaptic NMDA receptors. Activation of these receptors and release of Ca^{2+} from ryanodine-sensitive presynaptic stores are then sufficient to enhance GABAergic transmission. Although the same stimulation protocols (including climbing fiber stimulation) can induce both DSI[4,31,32] and DPI in the cerebellum, there are important differences between these forms of synaptic plasticity. First, DPI has a longer latency than DSI, reaching a peak after the termination of DSI and lasting several minutes before slowly subsiding. Second, different retrograde messengers are involved in their activation. Endocannabinoids cause a transient and rapid depression of Purkinje cell inhibitory inputs, whereas glutamate causes a longer-term facilitation of GABA release. This dual retrograde regulation of GABA release provides a mechanism for Purkinje cells to regulate their excitability dynamically after repetitive climbing fiber stimulation.

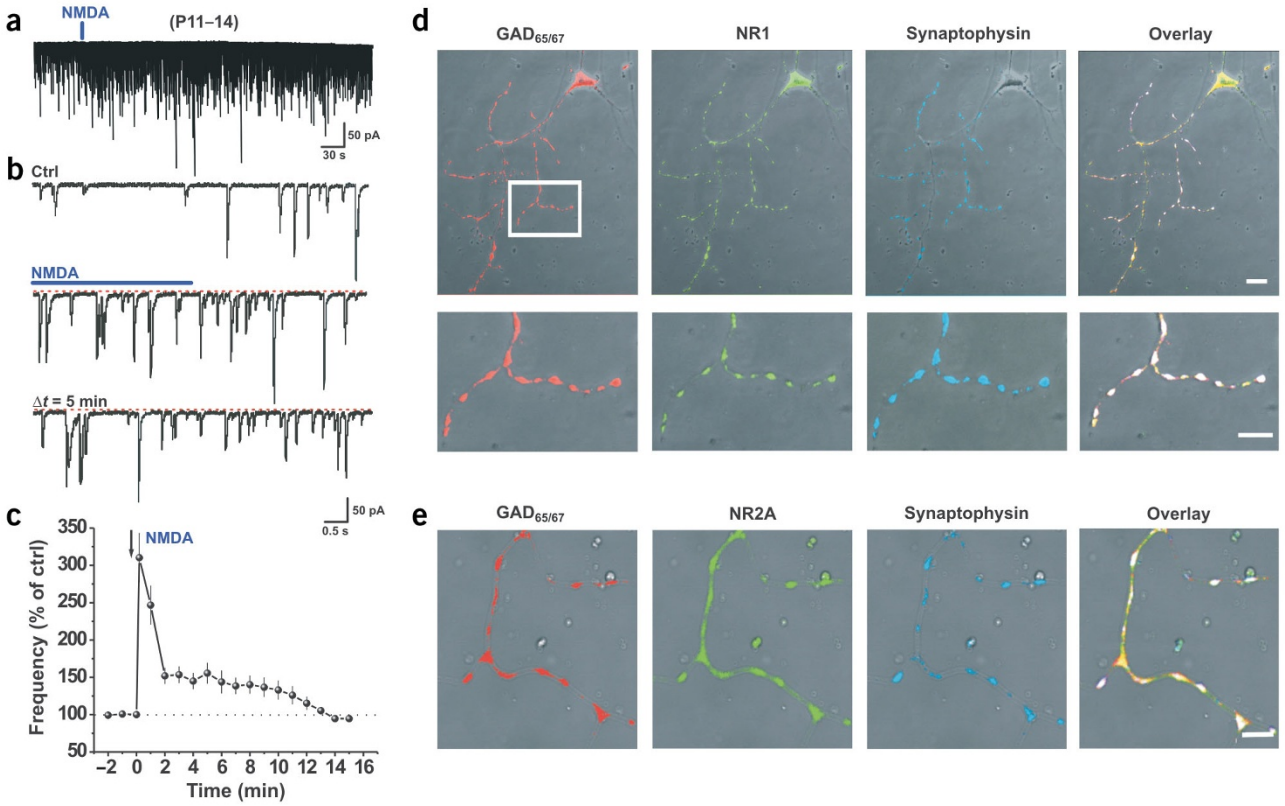

Figure 6 Brief activation of presynaptic NMDA receptors enhances IN-PC inhibitory synaptic transmission. (**a**) mIPSCs recorded from P11–14 Purkinje cells before, during (blue bar) and after a brief (4-s) focal application of 50 M NMDA. (**b**) Selected regions of **a** shown at higher time resolution for the control period (Ctrl), during NMDA application (blue bar) and 5 min after the NMDA pulse. The red dotted line represents the holding current level before NMDA application. (**c**) Normalized mean mIPSC frequencies before, during and after a 4-s pulse of NMDA (50 M, arrow) to P11–14 Purkinje cells ($n = 5$). (**d**) Upper, confocal images showing NR1 subunit (green), $GAD_{65/67}$ (red) and synaptophysin (blue) immunoreactivity throughout the soma and bifurcating axon of a cultured basket/stellate cell. Lower, high-power magnification of a section of the basket/stellate cell axon shown in the upper panels (white box) showing the abundance of NR1 subunits colocalized with both $GAD_{65/67}$ and synaptophysin. Extensive triple immunocolocalization was confined to the axon varicosities, which are presumed to be functionally mature transmitter release sites. (**e**) High-power magnification of a section of basket/stellate cell axon showing colocalization of NR2A subunits with both $GAD_{65/67}$ and synaptophysin. Scale bars, 10 m in upper panels of **d** and 5 m in lower panels of **d** and in **e**).

DPI relies on Ca^{2+}-dependent retrograde glutamate release

The requirement for increased stimulus durations to evoke DPI at later stages of cerebellar development (P11–14) revealed two important facets about this synaptic plasticity: its reliance on intracellular Ca^{2+} and on the extent of glial development. During early Purkinje cell development, Ca^{2+} binding markedly increased from P6 to P15 (ref. 43), which is attributable to an increased expression of calbindin D_{28K}[44]. Therefore, using similar stimulation protocols in P6–8 and P11–14 Purkinje cells will result in substantially different free Ca^{2+} concentrations that would affect Ca^{2+}-dependent synaptic plasticity. Presently, the induction of DSI (and DSE) requires postsynaptic Ca^{2+} to rise to ~15 M for half-maximal retrograde inhibition to occur[23,24]. Although requiring increments in postsynaptic Ca^{2+} levels for induction, the discrete signaling pathways for DSI[4,23,24,32] and DPI implies that these two mechanisms are not mutually exclusive in regulating GABA release.

An additional influence on DPI is the development of Bergmann glia, which increasingly encapsulate the Purkinje cell dendritic arbor, forming a physical barrier to the diffusion of transmitter from the synaptic cleft[45]. Bergmann glia express a high concentration of the glutamate transporter GLAST[46], which rapidly sequesters any released glutamate. This mechanism would limit the concentration of glutamate at presynaptic NMDA receptors. Thus, by increasing the stimulus intensity and facilitating glutamate release, we may transiently saturate the EAATs, allowing presynaptic NMDA receptor activation and consequently DPI induction. Therefore, by inhibiting glutamate uptake, we would expect—as we observed—to evoke a robust DPI after only modest Purkinje cell depolarization.

Presynaptic NMDA receptors

The absence of functional NMDA receptors in Purkinje cells, in conjunction with our observations that DPI is inhibited by D-APV and can be reproduced by applying NMDA, indicate that presynaptic NMDA receptors are involved in the induction of DPI. A presynaptic location for these receptors is suggested by three observations. First, to potentiate GABA transmission in the presence of TTX, the NMDA receptors mediating DPI are likely to be juxtaposed to the site(s) of glutamate release. This is probable because released glutamate will be rapidly sequestered by EAATs on Purkinje cell dendrites and Bergmann glia. Second, we observed a decrease in the paired-pulse ratio and an increase in $1/c.v.^2$, consistent with an increase in the probability of transmitter release at the IN-PC synapse. Third, our immunocytochemical data indicate the presence of both NR1 and NR2 subunits at putative presynaptic release sites on cerebellar bas-

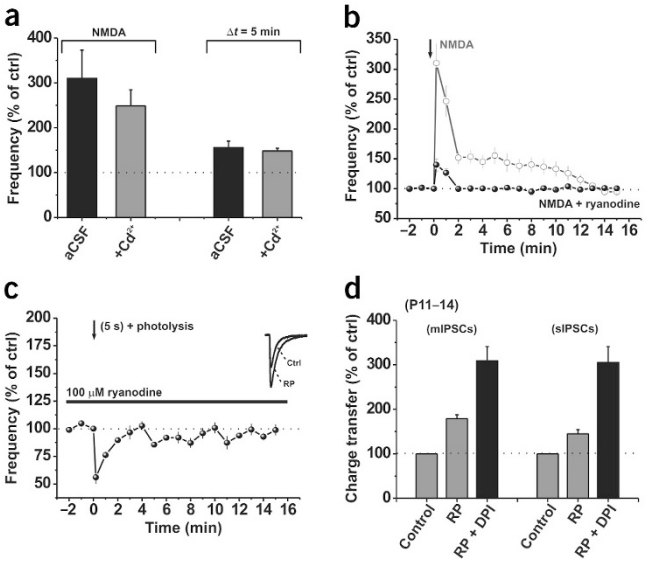

Figure 7 Presynaptic ryanodine-sensitive Ca^{2+} stores are required for DPI. (**a**) Bar graph of mIPSC frequencies during and 5 min after a 4-s pulse of NMDA (50 M) in the absence (black bars) and presence of 100 M Cd^{2+} (gray bars, $n = 5$). (**b**) Effect of inhibiting ryanodine-sensitive presynaptic Ca^{2+} stores (ryanodine, 100 M) on the modulation of mIPSC frequency caused by the focal application (arrow) of NMDA (50 M) in P11–14 Purkinje cells (black circles, $n = 5$). The effects of NMDA on mIPSC frequency in the absence of ryanodine (open circles) are reproduced from **Fig. 6c** for comparison. (**c**) Normalized mean mIPSC frequencies recorded in the presence of ryanodine (black bar, 100 M) before and after application of a conditioning stimulus to compensate for the postsynaptic effects of ryanodine. This consisted of a 5-s depolarization concurrent with the rapid photolysis of nitrophenyl EGTA (three 1-ms flashes). Inset, superimposed examples of mean mIPSCs (from 50 consecutive events) recorded in control and 5 min after the compensated conditioning stimuli (rebound potentiation, RP; $n = 5$). (**d**) DPI enhances synaptic efficacy at the IN-PC synapse. Comparison of the relative charge transfer measured during 60-s epochs in control, after induction of RP alone, and after induction of RP and DPI at the IN-PC synapse ($n = 5$–8).

ket/stellate cells. Notably, the NMDA receptor activation occurs even in the presence of 1 mM Mg^{2+}, without any pre-depolarization to remove the voltage-dependent Mg^{2+} block. There are two possible reasons why presynaptic NMDA receptors might be activated under such conditions. First, NMDA receptors composed of NR1 and NR2C or NR2D subunits are less sensitive to Mg^{2+} blockade than their NR1 and NR2A counterparts and are thus capable of activation at more negative membrane potentials[47]. Second, the high input resistance and small volume of interneuron axon terminals implies that only a very small glutamate-activated current would be necessary to depolarize the terminal and relieve the Mg^{2+} block, allowing the induction of DPI. Therefore, DPI, with its reliance on presynaptic NMDA receptors, is a mechanism that can enhance inhibitory transmitter release even without the need for coincident presynaptic action potential activity.

Role of presynaptic Ca^{2+} stores in synaptic plasticity

Depolarization of Purkinje cells induced a strong enhancement of synaptic efficacy that affected both action potential–dependent and –independent forms of inhibitory transmission. Therefore, it is likely that DPI affects the GABA release process at the level of presynaptic Ca^{2+} stores by a CICR mechanism, rather than relying solely on Ca^{2+} influx through the NMDA receptors, given the ability of ryanodine to block DPI completely. The support of DPI by CICR in individual boutons may occur after either an increase in the frequency of spontaneous Ca^{2+} transients, NMDA receptor activation or an initial discrete presynaptic Ca^{2+} signal that is sufficient to trigger a sustained increase in the transmitter release process. Thus, although presynaptic Ca^{2+} stores can contribute to spontaneous[38] and evoked[48] GABA release, they are pivotal to the induction of inhibitory synaptic plasticity at the IN-PC synapse.

DPI enhances GABAergic synaptic efficacy

Our data suggest that Purkinje cells can release glutamate after depolarization, providing a new feedback mechanism to enhance inhibitory synaptic strength over several minutes (see **Supplementary Fig. 1** online). An important effect of synaptic inhibition is to provide an increased membrane Cl^- conductance that 'shunts' excitatory currents. This synaptic GABA-activated conductance will depend on the charge transfer across the membrane. In this regard, the functional consequences of DPI were recognized by examining the synaptic charge transfer during DPI and rebound potentiation. The coincident activation of these two independent plasticity mechanisms markedly increased the charge transfer and overall inhibitory synaptic efficacy at the IN-PC synapse for several tens of minutes. Therefore, glutamate retrograde signaling provides a specific, distinctive mechanism whereby Purkinje cells can alter the strength and properties of their synaptic inputs after periods of postsynaptic stimulation. This mechanism of inhibitory synaptic plasticity may have more generalized implications for synaptic inhibition in the CNS.

METHODS

Slices. Thin sagittal cerebellar slices (200 m thick) were cut from P6–8 or P11–14 Sprague-Dawley rats using a Leica VT1000S vibroslicer. Slices were cut at 2–4 °C in artificial CSF solution (aCSF) containing (mM) 125 NaCl, 2.5 KCl, 1.25 NaH_2PO_4, 25 $NaHCO_3$, 2 $CaCl_2$, 1 $MgCl_2$ and 10 glucose bubbled with 95% O_2/5% CO_2. The slices were then incubated at 35 °C for 45 min before being allowed to cool to room temperature (22–25 °C) before use. Slices were perfused in the recording bath at 1 ml/min with aCSF at 32 °C.

Electrophysiology. Membrane currents were recorded with a MultiClamp 700A (Axon Instruments) and filtered at 3 kHz (Bessel, 8 pole, –36 dB per octave). During most recordings, Purkinje cells were voltage clamped at –70 mV. For direct Purkinje cell stimulation, patch pipettes (3–5 MΩ) were filled with a solution containing (mM) 150 CsCl, 1.5 $MgCl_2$, 10 HEPES, 0.1 cesium BAPTA, 2 sodium ATP, 0.4 sodium GTP, 5 QX-314 (to block Na^+ action potentials) at pH 7.3. The Ca^{2+} buffer BAPTA (30 mM) was included to allow examination of the Ca^{2+} dependence of DPI. For current-clamp experiments or when using climbing fiber stimulation, the pipette solution contained (mM) 105 potassium acetate, 25 KCl, 10 NaCl, 2 $MgCl_2$, 0.16 $CaCl_2$, 0.5 EGTA, 20 HEPES, 2 sodium ATP, 0.4 sodium GTP at pH 7.3. For the photolytic Ca^{2+} release experiments, patch electrodes were filled with (mM):150 CsCl, 3 $MgCl_2$, 10 HEPES, 4 nitrophenyl-EGTA, 2.4 $CaCl_2$, 2 sodium ATP, 0.4 sodium GTP at pH 7.3. To uncage nitrophenyl-EGTA, cells were irradiated three times, separated by intervals of 2.5 s, with a 1-ms pulse of near-UV light (260–370 nm with a UV-2 filter) from a short-arc xenon flash lamp (JML-C2 system, Rapp-Optoelectronic, Germany).

The induction of DSI, DPI and rebound potentiation was initiated with a conditioning stimulus applied 5 min after the whole-cell configuration was attained. This entailed stepping the membrane potential from –70 mV to 0 mV for a total duration of 0.8 s (eight 100-ms pulses; 0.5 Hz); 2 s (2,000 ms, 1 stimulus); or 5 s (5,000 ms, 1 stimulus). Climbing fiber EPSCs were evoked by placing a stimulating electrode filled with aCSF in the granular layer ~20 m from the recorded Purkinje cell and applying a short (0.2-ms) stimulus of 1–10 V in the absence of TTX and NBQX. All drugs were bath applied, except NMDA, which was pressure-applied. Ryanodine, NMDA and cesium BAPTA were obtained from Sigma and LY341495, D-APV, $CdCl_2$, TTX, THA and QX-314 from Tocris.

Synaptic current analyses. Spontaneous, miniature and evoked IPSCs were measured and analyzed offline using MiniAnalysis version 6 (Synaptosoft) or Clampfit 8.2 (Axon Instruments). To calculate the mean paired-pulse ratio (PPR) from IPSC amplitudes (amp), 20–30 paired evoked IPSCs were recorded for DPI (8 for DSI). The PPR was then calculated as mean $ampIPSC_2$/mean $ampIPSC_1$. This method of calculating the PPR at inhibitory synapses prevented bias that could result from IPSC amplitude fluctuations[49]. The c.v. of the IPSC amplitudes was calculated as c.v. = s.d./m, where m is the mean and s.d. the standard deviation of IPSC amplitudes.

DSI was calculated as the percentage change in IPSC frequency during the initial 20s after stimulus cessation. DPI was measured as the peak percentage change in IPSC frequency after termination of DSI (1–20 min). Rebound potentiation was calculated as the percentage change in IPSC amplitude over 1–20 min after stimulus cessation. The synaptic charge transfer was determined by integrating the total areas of 60-s epochs of IPSCs under control conditions and 5 min after stimulus during the peaks of DPI and rebound potentiation. The charge transfers were normalized to the controls. All values in the text are provided as mean ± s.e.m. Statistical significance was examined using Student's paired t-test or by a one-way ANOVA with a Bonferroni post-test where $P < 0.05$ was considered significant.

Immunocytochemistry. Cerebellar cultures were fixed in phosphate-buffered saline (PBS) with 4% paraformaldehyde before being quenched with 50 mM NH_4Cl in PBS. Cells were permeabilized using 10% fetal calf serum (FCS), 0.5% bovine serum albumin (BSA), 0.1% Triton X in PBS. Cultures were incubated with primary antibody for 30 min, washed in FCS and BSA in PBS solution before being incubated at room temp for 30 min with a single secondary antibody conjugate or an antibody conjugate mixture. Presynaptic NMDA receptor distribution used a primary antibody mixture containing goat anti-$GAD_{65/67}$ (Swant), rabbit anti-NR1 or anti-NR2A-D, mouse anti-synaptophysin (Biomeda Corporation) and a secondary conjugate mixture containing anti-goat–TRITC, anti-rabbit–FITC and anti-mouse–Cy5 (Stratech Scientific). Mounted slides of cultures were viewed using an upright Leica DMRE laser-scanning microscope and confocal images were obtained from a Leica TCS SP spectrophotometer.

Note: Supplementary information is available on the Nature Neuroscience website.

ACKNOWLEDGMENTS

We thank A. Gibb, B. Clark, A. Hosie and P. Thomas for helpful discussions on the manuscript. This work was supported by the Biotechnology and Biological Sciences Research Council, Medical Research Council and GlaxoSmithKline. We thank S. Moss (University College London) for the NR1 antibody, P. Whiting (Merck, Sharp and Dohme) for the NR2 antibodies, D. Baker (Institute of Neurology, University College London) for SR141716A and T. Carter (National Institute for Medical Research) for the nitrophenyl-EGTA.

COMPETING INTERESTS STATEMENT

The authors declare that they have no competing financial interests.

Received 24 November 2003; accepted 22 March 2004
Published online at http://www.nature.com/natureneuroscience/

1. Llano, I., Leresche, N. & Marty, A. Calcium entry increases the sensitivity of cerebellar Purkinje cells to applied GABA and decreases inhibitory synaptic currents. *Neuron* **6,** 565–574 (1991).
2. Pitler, T.A. & Alger, B.E. Postsynaptic spike firing reduces synaptic $GABA_A$ responses in hippocampal pyramidal cells. *J. Neurosci.* **12,** 4122–4132 (1992).
3. Ohno-Shosaku, T., Maejima, T. & Kano, M. Endogenous cannabinoids mediate retrograde signals from depolarized postsynaptic neurons to presynaptic terminals. *Neuron* **29,** 729–738 (2001).
4. Kreitzer, A.C. & Regehr, W.G. Cerebellar depolarization-induced suppression of inhibition is mediated by endogenous cannabinoids. *J. Neurosci.* **21,** RC174–RC1745 (2001).
5. Kreitzer, A.C. & Regehr, W.G. Retrograde inhibition of presynaptic calcium influx by endogenous cannabinoids at excitatory synapses onto Purkinje cells. *Neuron* **29,** 717–727 (2001).
6. Takahashi, K.A. & Linden, D.J. Cannabinoid receptor modulation of synapses received by cerebellar Purkinje cells. *J. Neurophysiol.* **83,** 1167–1180 (2000).
7. Wilson, R.I. & Nicoll, R.A. Endogenous cannabinoids mediate retrograde signalling at hippocampal synapses. *Nature* **410,** 588–592 (2001).
8. Zilberter, Y., Kaiser, K.M. & Sakmann, B. Dendritic GABA release depresses excitatory transmission between layer 2/3 pyramidal and bitufted neurons in rat neocortex. *Neuron* **24,** 979–988 (1999).
9. Pittman, Q.J., Hirasawa, M., Mouginot, D. & Kombian, S.B. Neurohypophysial peptides as retrograde transmitters in the supraoptic nucleus of the rat. *Exp. Physiol.* **85** (Spec No.), 139S–143S (2000).
10. Zilberter, Y. Dendritic release of glutamate suppresses synaptic inhibition of pyramidal neurons in rat neocortex. *J. Physiol. (Lond.)* **528,** 489–496 (2000).
11. Levenes, C., Daniel, H. & Crepel, F. Retrograde modulation of transmitter release by postsynaptic subtype 1 metabotropic glutamate receptors in the rat cerebellum. *J. Physiol. (Lond.)* **537,** 125–140 (2001).
12. Yung, W.H. *et al.* Secretin facilitates GABA transmission in the cerebellum. *J. Neurosci.* **21,** 7063–7068 (2001).
13. Petralia, R.S., Wang, Y.X. & Wenthold, R.J. The NMDA receptor subunits NR2A and NR2B show histological and ultrastructural localization patterns similar to those of NR1. *J. Neurosci.* **14,** 6102–6120 (1994).
14. DeBiasi, S., Minelli, A., Melone, M. & Conti, F. Presynaptic NMDA receptors in the neocortex are both auto- and heteroreceptors. *Neuroreport* **7,** 2773–2776 (1996).
15. Casado, M., Isope, P. & Ascher, P. Involvement of presynaptic *N*-methyl-D-aspartate receptors in cerebellar long-term depression. *Neuron* **33,** 123–130 (2002).
16. Glitsch, M. & Marty, A. Presynaptic effects of NMDA in cerebellar Purkinje cells and interneurons. *J. Neurosci.* **19,** 511–519 (1999).
17. Ito, M. *The Cerebellum and Neural Control* (Raven Press, New York, 1984).
18. Armstrong, D.M. & Rawson, J.A. Activity patterns of cerebellar cortical neurones and climbing fibre afferents in the awake cat. *J. Physiol. (Lond.)* **289,** 425–448 (1979).
19. Kano, M., Rexhausen, U., Dreessen, J. & Konnerth, A. Synaptic excitation produces a long-lasting rebound potentiation of inhibitory synaptic signals in cerebellar Purkinje cells. *Nature* **356,** 601–604 (1992).
20. Konnerth, A., Dreessen, J. & Augustine, G.J. Brief dendritic calcium signals initiate long-lasting synaptic depression in cerebellar Purkinje cells. *Proc. Natl. Acad. Sci. USA* **89,** 7051–7055 (1992).
21. Miyakawa, H., Lev-Ram, V., Lasser-Ross, N. & Ross, W.N. Calcium transients evoked by climbing fiber and parallel fiber synaptic inputs in guinea pig cerebellar Purkinje neurons. *J. Neurophysiol.* **68,** 1178–1189 (1992).
22. Hashimoto, T., Ishii, T. & Ohmori, H. Release of Ca^{2+} is the crucial step for the potentiation of IPSCs in the cultured cerebellar Purkinje cells of the rat. *J. Physiol. (Lond.)* **497,** 611–627 (1996).
23. Brenowitz, S.D. & Regehr, W.G. Calcium dependence of retrograde inhibition by endocannabinoids at synapses onto Purkinje cells. *J. Neurosci.* **23,** 6373–6384 (2003).
24. Brown, S.P., Brenowitz, S.D. & Regehr, W.G. Brief presynaptic bursts evoke synapse-specific retrograde inhibition mediated by endogenous cannabinoids. *Nature Neurosci.* **6,** 1048–1057 (2003).
25. Sotelo, C. & Wassef, M. Cerebellar development: afferent organization and Purkinje cell heterogeneity. *Phil. Trans. R. Soc. Lond. B Biol. Sci.* **331,** 307–313 (1991).
26. Strata, P., Tempia, F., Zagrebelsky, M. & Rossi, F. Reciprocal trophic interactions between climbing fibres and Purkinje cells in the rat cerebellum. *Prog. Brain Res.* **114,** 263–282 (1997).
27. Knopfel, T., Vranesic, I., Staub, C. & Gahwiler, B.H. Climbing fibre responses in olivo-cerebellar slice cultures. II. Dynamics of cytosolic calcium in Purkinje cells. *Eur. J. Neurosci.* **3,** 343–348 (1991).
28. Hashimoto, K. & Kano, M. Presynaptic origin of paired-pulse depression at climbing fibre-Purkinje cell synapses in the rat cerebellum. *J. Physiol. (Lond.)* **506,** 391–405 (1998).
29. Silver, R.A., Momiyama, A. & Cull-Candy, S.G. Locus of frequency-dependent depression identified with multiple-probability fluctuation analysis at rat climbing fibre-Purkinje cell synapses. *J. Physiol. (Lond.)* **510,** 881–902 (1998).
30. Pouzat, C. & Hestrin, S. Developmental regulation of basket/stellate cell–Purkinje cell synapses in the cerebellum. *J. Neurosci.* **17,** 9104–9112 (1997).
31. Yoshida, T. *et al.* The cannabinoid CB1 receptor mediates retrograde signals for depolarization-induced suppression of inhibition in cerebellar Purkinje cells. *J. Neurosci.* **22,** 1690–1697 (2002).
32. Diana, M.A., Levenes, C., Mackie, K. & Marty, A. Short-term retrograde inhibition of GABAergic synaptic currents in rat Purkinje cells is mediated by endogenous cannabinoids. *J. Neurosci.* **22,** 200–208 (2002).
33. Glitsch, M., Llano, I. & Marty, A. Glutamate as a candidate retrograde messenger at interneurone-Purkinje cell synapses of rat cerebellum. *J. Physiol. (Lond.)* **497,** 531–537 (1996).
34. Rosenmund, C., Legendre, P. & Westbrook, G.L. Expression of NMDA channels on cerebellar Purkinje cells acutely dissociated from newborn rats. *J. Neurophysiol.* **68,** 1901–1905 (1992).
35. Paquet, M. & Smith, Y. Presynaptic NMDA receptor subunit immunoreactivity in GABAergic terminals in rat brain. *J. Comp. Neurol.* **423,** 330–347 (2000).
36. Stephens, G.J., Morris, N.P., Fyffe, R.E. & Robertson, B. The Cav2.1/αA (P/Q-type) voltage-dependent calcium channel mediates inhibitory neurotransmission onto mouse cerebellar Purkinje cells. *Eur. J. Neurosci.* **13,** 1902–1912 (2001).
37. Mayer, M.L., Vyklicky, L., Jr. & Westbrook, G.L. Modulation of excitatory amino acid receptors by group IIB metal cations in cultured mouse hippocampal neurones. *J. Physiol. (Lond.)* **415,** 329–350 (1989).
38. Llano, I. *et al.* Presynaptic calcium stores underlie large-amplitude miniature IPSCs and spontaneous calcium transients. *Nature Neurosci.* **3,** 1256–1265 (2000).
39. Emptage, N.J., Reid, C.A. & Fine, A. Calcium stores in hippocampal synaptic boutons mediate short-term plasticity, store-operated Ca^{2+} entry, and spontaneous transmitter release. *Neuron* **29,** 197–208 (2001).

40. Zucker, R. S. Calcium- and activity-dependent synaptic plasticity. *Curr. Opin. Neurobiol.* **9,** 305–313 (1999).
41. Zimanyi, I., Buck, E., Abramson, J.J., Mack, M.M. & Pessah, I.N. Ryanodine induces persistent inactivation of the Ca^{2+} release channel from skeletal muscle sarcoplasmic reticulum. *Mol. Pharmacol.* **42,** 1049–1057 (1992).
42. Kano, M., Kano, M., Fukunaga, K. & Konnerth, A. Ca^{2+}-induced rebound potentiation of γ-aminobutyric acid-mediated currents requires activation of Ca^{2+}/calmodulin-dependent kinase II. *Proc. Natl. Acad. Sci. USA* **93,** 13351–13356 (1996).
43. Fierro, L. & Llano, I. High endogenous calcium buffering in Purkinje cells from rat cerebellar slices. *J. Physiol. (Lond.)* **496,** 617–625 (1996).
44. Kurobe, N. *et al.* Developmental and age-dependent changes of 28-kDa calbindin-D in the central nervous tissue determined with a sensitive immunoassay method. *J. Neurochem.* **58,** 128–134 (1992).
45. Yamada, K. *et al.* Dynamic transformation of Bergmann glial fibers proceeds in correlation with dendritic outgrowth and synapse formation of cerebellar Purkinje cells. *J. Comp. Neurol.* **418,** 106–120 (2000).
46. Yamada, K. & Watanabe, M. Cytodifferentiation of Bergmann glia and its relationship with Purkinje cells. *Anat. Sci. Int.* **77,** 94–108 (2002).
47. Monyer, H., Burnashev, N., Laurie, D.J., Sakmann, B. & Seeburg, P. H. Developmental and regional expression in the rat brain and functional properties of four NMDA receptors. *Neuron* **12,** 529–540 (1994).
48. Galante, M. & Marty, A. Presynaptic ryanodine-sensitive calcium stores contribute to evoked neurotransmitter release at the basket cell-Purkinje cell synapse. *J. Neurosci.* **23,** 11229–11234 (2003).
49. Kim, J. & Alger, B.E. Random response fluctuations lead to spurious paired-pulse facilitation. *J. Neurosci.* **21,** 9608–9618 (2001).